AD-A132 914 ANALYSIS OF SNOW CHARACTERIZATION DATA ACQUIRED AT SNOW-ONE-A!AND B(U) AIR FORCE GEOPHYSICS LAB HANSCOM AFB MA R O BERTHEL ET AL. 08 SEP 83 AFGL-TR-83-0222 1/1

UNCLASSIFIED F/G 8/12 NL

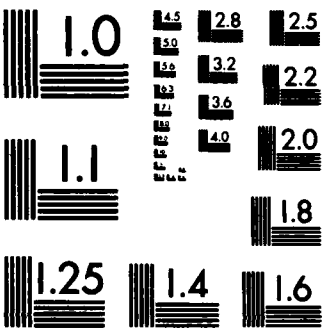

Unclassified

SECURITY CLASSIFICATION OF THIS PAGE

AD-A132 914

REPORT DOCUMENTATION PAGE

1a. REPORT SECURITY CLASSIFICATION: Unclassified	1b. RESTRICTIVE MARKINGS
2a. SECURITY CLASSIFICATION AUTHORITY	3. DISTRIBUTION/AVAILABILITY OF REPORT: Approved for Public Release; Distribution Unlimited
2b. DECLASSIFICATION/DOWNGRADING SCHEDULE	
4. PERFORMING ORGANIZATION REPORT NUMBER(S): AFGL-TR-83-0222	5. MONITORING ORGANIZATION REPORT NUMBER(S)
6a. NAME OF PERFORMING ORGANIZATION: Air Force Geophysics Laboratory; 6b. OFFICE SYMBOL (If applicable): LYC	7a. NAME OF MONITORING ORGANIZATION
6c. ADDRESS (City, State and ZIP Code): Hanscom AFB, MA 01731	7b. ADDRESS (City, State and ZIP Code)
8a. NAME OF FUNDING/SPONSORING ORGANIZATION; 8b. OFFICE SYMBOL (If applicable)	9. PROCUREMENT INSTRUMENT IDENTIFICATION NUMBER
8c. ADDRESS (City, State and ZIP Code)	10. SOURCE OF FUNDING NOS.

PROGRAM ELEMENT NO.	PROJECT NO.	TASK NO.	WORK UNIT NO.
62101F	6670	12	02

11. TITLE (Include Security Classification) (U) Analysis of Snow Characterization Data Acquired at SNOW-ONE-A & B

12. PERSONAL AUTHOR(S): Robert O. Berthel, Vernon G. Plank, Barbara A. Main

13a. TYPE OF REPORT	13b. TIME COVERED	14. DATE OF REPORT (Yr., Mo., Day)	15. PAGE COUNT
REPRINT	FROM _____ TO _____	1983 Sep 8	12

16. SUPPLEMENTARY NOTATION: Presented at Snow Symposium III, U.S. Army Corp of Engineers, CRREL, Hanover, NH, 9-11 August 1983

17. COSATI CODES		
FIELD	GROUP	SUB. GR.

18. SUBJECT TERMS (Continue on reverse if necessary and identify by block number): SNOW-ONE-A; SNOW-ONE-B; Fall Velocity; Crystal Identification; Snow Rate

19. ABSTRACT (Continue on reverse if necessary and identify by block number)

Snow characterization measurements acquired by the snow rate meter, fall-velocity indicator and snow-structure recorder obtained during the SNOW-ONE-B field experiment are presented. Some further analyses of the SNOW-ONE-A data are also given. Correlations between snow rates, electro-optical and liquid-water-content measurements are shown with the relationships of fall velocities with these parameters are discussed.

20. DISTRIBUTION/AVAILABILITY OF ABSTRACT	21. ABSTRACT SECURITY CLASSIFICATION
UNCLASSIFIED/UNLIMITED ☐ SAME AS RPT. ☒ DTIC USERS ☐	Unclassified

22a. NAME OF RESPONSIBLE INDIVIDUAL	22b. TELEPHONE NUMBER (Include Area Code)	22c. OFFICE SYMBOL
Diane Corazzini	(617) 861-4553	AFGL/SULR

DD FORM 1473, 83 APR EDITION OF 1 JAN 73 IS OBSOLETE.

Unclassified

SECURITY CLASSIFICATION OF THIS PAGE

AFGL-TR-83-0222

ANALYSIS OF SNOW CHARACTERIZATION DATA ACQUIRED AT SNOW-ONE-A AND B

Robert O. Berthel
Vernon G. Plank
Barbara A. Main

Cloud Physics Branch (LYC),
Meteorology Division
Air Force Geophysics Laboratory
Hanscom AFB, MA 01731

ABSTRACT

Snow characterization measurements acquired by the snow rate meter, fall-velocity indicator and snow-structure recorder obtained during the SNOW-ONE-B field experiment are presented. Some further analyses of the SNOW-ONE-A data are also given. Correlations between snow rates, electro-optical and liquid-water-content measurements are shown and the relationships of fall velocities with these parameters are discussed.

1. INTRODUCTION

AFGL snow characterization efforts during both SNOW-ONE-A and SNOW-ONE-B were concentrated on three objectives: the determination of crystal type using a snow-structure recorder (SSR), the measurement of snow rate with a snow-rate meter (SRM) and the measurement of fall velocity using a fall-velocity indicator (FVI). Descriptions of these instruments, methods of operations and data obtained have been previously reported in the SNOW-ONE-A Data Report (Berthel, 1982); SNOW-ONE-B Data Report (Berthel, et. al., 1983); at SNOW Symposium II (Berthel, et. al., 1982); at the SPIE Symposium (Plank, et. al., 1983) and in a AFGL report (Gibbons, et. al., 1983). This paper is primarily concerned with the presentation of additional data analyses on one day of each experiment, namely the 31 Jan 82 of SNOW-ONE-A and 12 Dec 82 of SNOW-ONE-B.

2. SNOW-ONE-A Field Experiment (31 Jan 82)

All instruments were operating during the 31 Jan 82 storm. Measurements from the FVI taken during brief periods of each hourly "Intensive Measurement Period" (IMP) are shown in the fall velocity vs size (ℓ is the largest physical dimension) plot in Fig. 1. The time-consuming labor required for the reduction of these data prevented a complete analysis, thus only a representative sample (~ 30 measurements) from each IMP from 1600 through 2000 EST were initially analyzed. Little data were recorded after ~ 2000 EST because of an increase in winds (Bates, 1982; Olsen, et.al., 1982). The solid line in the figure is the least-squares-regression line obtained from these data and the dashed lines show plus or minus one standard deviation.

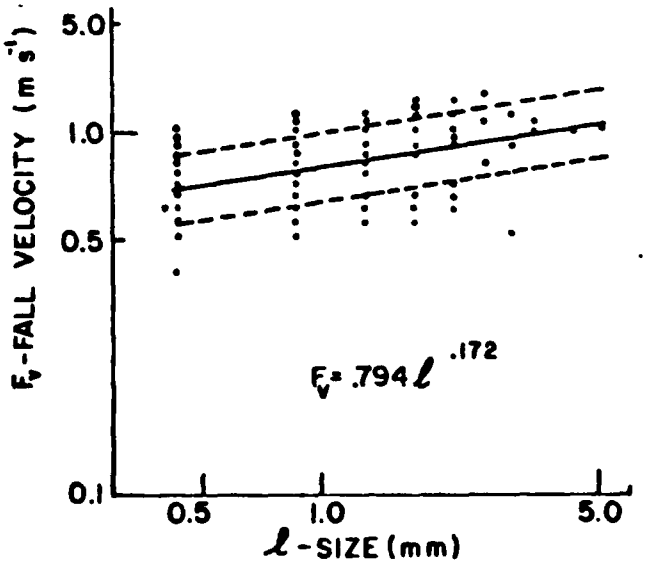

Fig. 1 Fall velocities of individual particles on 31 Jan 82.

Inherent uncertainties exist in these data because of instrument collection efficiency, video resolution and analyst subjectivity. The measurements may not be representative in respect to the number and sizes of the natural snowfall distribution because of wind effects and the small sampling volume. Some particles, most noticeably the smaller ones, reflect less light and result in faded video images. This, in combination with limited video resolution and image magnification, often prevents the analyst from determining if a particle is tumbling or turning thus, the measurement of fall distance may not be made on the same part of the falling snowflake. An apparent large scatter in fall velocities can result because of such uncertainties in fall distance. Similar effects may be present in the determination of the largest particle dimensions. These uncertainties may be mitigated by considering an averaged-fall velocity vs size relationship that should give more meaningful comparisons with other data analyzed in the same manner.

The fall velocity data presented in Fig. 1 were processed so that the number of particles within class limits of 0.5 mm were averaged to give the mean-fall velocity and ℓ for each class. These values were then regressed as per the solid line in Fig. 2.

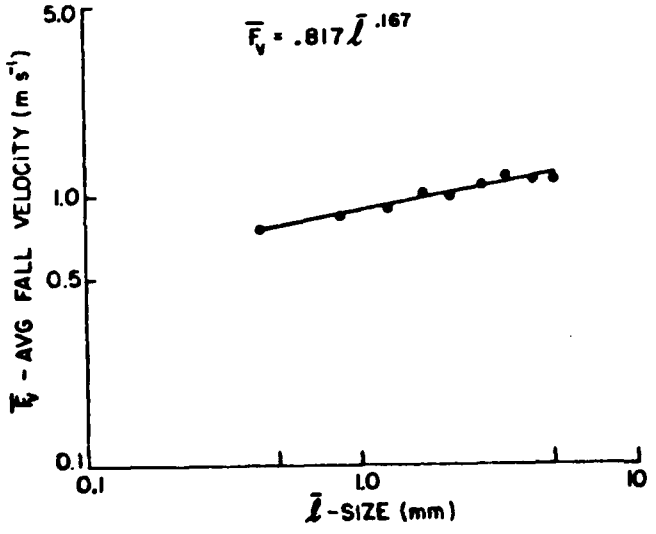

Fig. 2 Class-averaged-fall velocities on 31 Jan 82.

Although this type analysis provides a more useful relationship for comparison purposes than that of Fig. 1, the data presented in both Figs. 1 and 2 are from discrete periods taken hourly throughout the storm, thus more comprehensive analyses are needed for each IMP as the fall velocity vs size relationships will probably vary with changes in crystal type.

An in-depth analysis was performed on the 1900 EST IMP for 31 Jan 82. We divided the 20 minute period into 4 discrete entities with start times of 1900, 1905, 1910 and 1915 EST. The first 100 particles of each period (~ 1 minute of data) were measured and subjected to a regression analysis using the class-averaged-fall velocities. The plots and resulting equations for these four 1 minute periods are presented in Fig. 3.

It is interesting to note that the velocity - size relationships of the first 3 plots show little variation, which implies that the snow crystal type remained fairly consistant at least throughout the initial 11 minutes of the IMP. The difference between these plots and those of Fig. 2, the plot covering the 1600 through 2000 EST IMPs, infers that some changes in the nature of the snow crystals occurred during that portion of the storm.

The SSR produced some data on this day although the quality was not up to expectation. The particular instrument design used during SNOW-ONE-A employed a continuously moving belt utilizing strobe lighting to provide "stop action". Two detrimental effects of this configuration were noted. First, the flash rate had to be synchronized with the speed of the belt to avoid multiple images on a single video frame. Second, the intense flash-tube light produced reflections from the snow crystals which tended to cause blurred images. Thus, the data could not contribute to the analysis.

CRREL operated three ASMCE Instruments during SNOW-ONE-A (Lacombe, J., 1982). A scatter diagram showing the correlation of the CRREL mass-concentration measurements (M) for instrument No. 1 versus the AFGL snow-rate (of precipitation rate, P) values for 31 Jan 82 are shown in Fig. 4. The SRM data were averaged over 1 minute periods to conform with the ASCME 1 minute data. The power function equation and coefficient of correlation from the least-squares regression are listed. (This equation has a slightly different coefficient and exponent than previously reported at the SPIE Symposium. The initial analysis used 2.81 second SRM data that were averaged +/- 30 seconds from the even 1 minute times. This regression uses SRM data averaged over the 60 seconds preceding the 1 minute time. We believe that this method conforms better

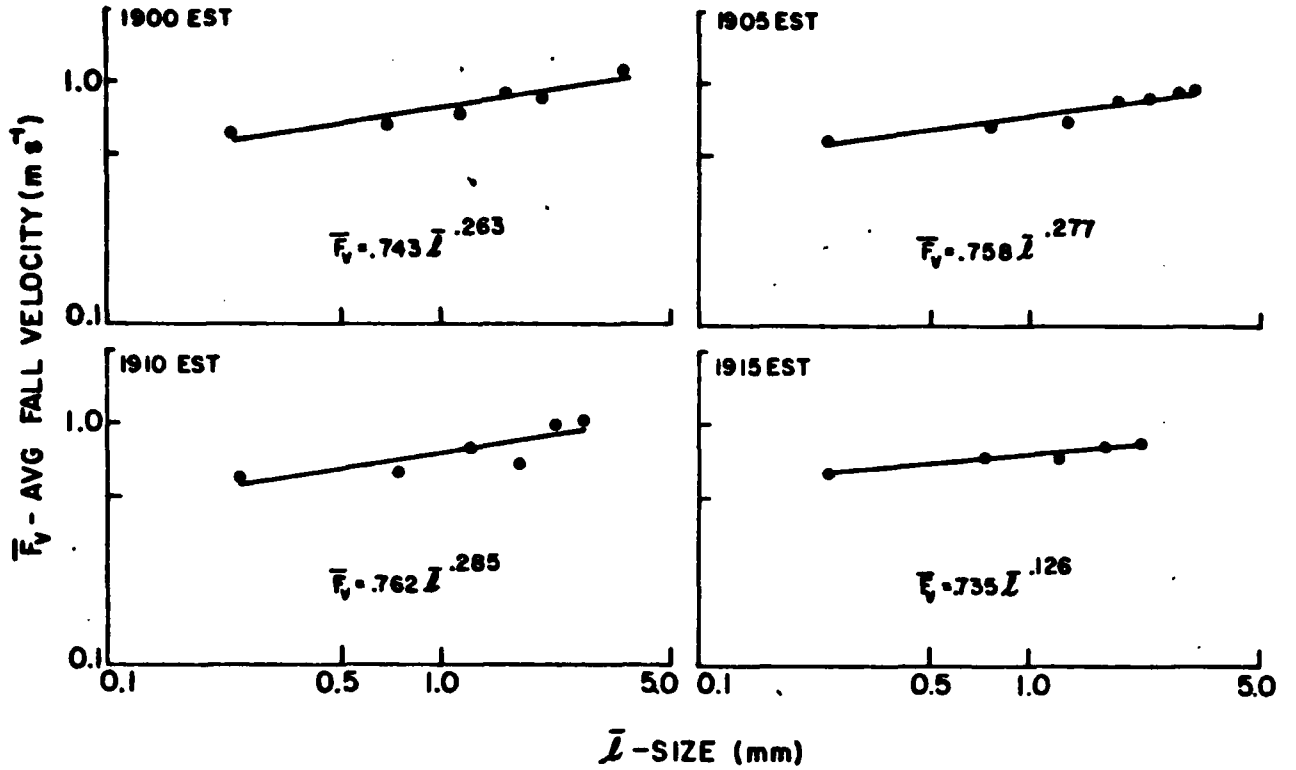

Fig. 3 Class-averaged-fall velocities from the 1900 EST IMP on 31 Jan 82.

with the measurements obtained by the ASCME.) This plot reveals that the correlation is best for the largest mass concentrations and snow-rate values and that the scatter increases as the M and P becomes smaller.

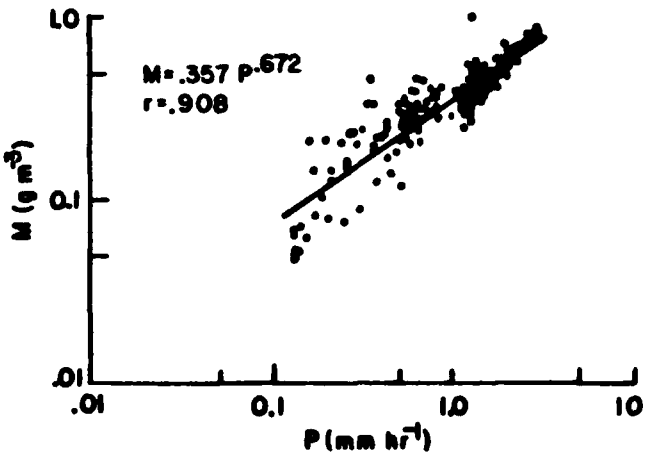

Fig. 4 Correlation of mass concentration (M) and snow rate (P) for ASCME No. 1 on 31 Jan 82.

As a means of reducing the scatter, we applied a five-point-running mean to both the ASCME No.1 and SRM data used in Fig. 4. The scatter diagram and regression line (solid line) of these averaged data are shown in Fig. 5. The suppression of the scatter gives results that show two distinct M vs P trends as shown by the dashed lines.

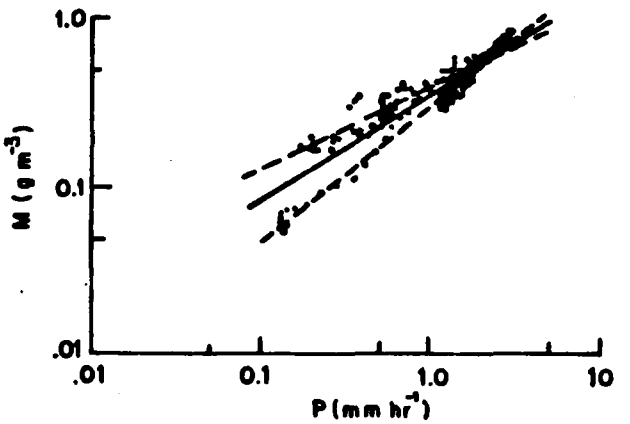

Fig. 5 Correlation of M and P using 5 minute averaging for ASCME No. 1 on 31 Jan 82.

When viewing the time-resolved, mass concentration and snow-rate data it is apparent that the 5 minute points showing the most scatter are from the data obtained during the period of light snowfall beginning at ~ 2010 EST. The data were divided at this time into two separate sets; the first spanning 1610 to 2010 EST and the second, 2010 to 2135 EST. The M-P plots, least-square-regression lines and equations for ASCME No. 1 data from these two time periods are shown in Figs. 6. The regression equations from the two periods differ considerably from one to another and with the complete data set of Fig. 4 This suggests the possibil-

ity that a change in the nature of the snowfall occurred at about 2000 EST.

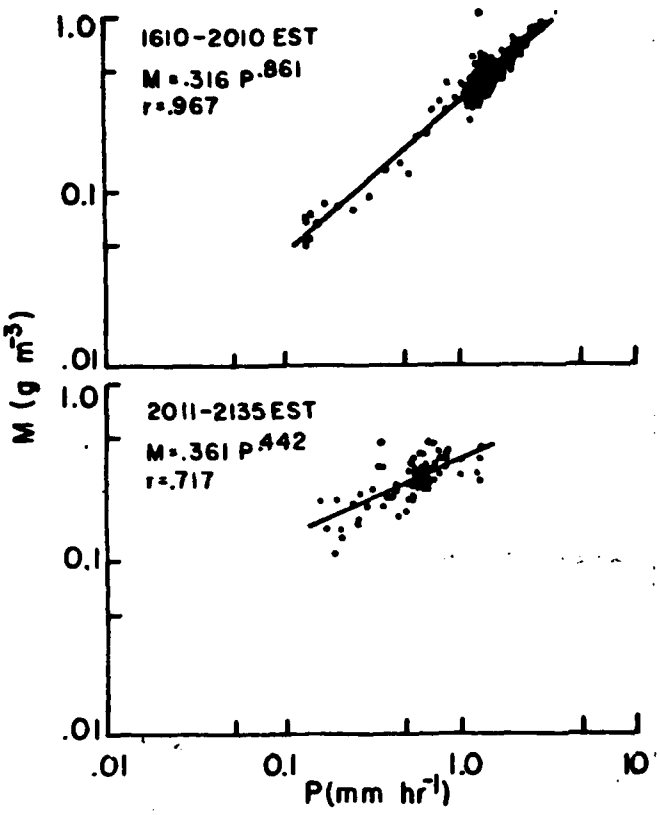

Fig. 6 Correlation of M and P for ASCME No. 1 from 1610 to 2010 EST and from 2011 to 2135 EST on 31 Jan 82.

Koh and O'Brien (1982) of CRREL monitored crystal habit by Formvar replication during the storm of 31 Jan 82. They observed at 1910 EST, "orthogonally intersecting broad-branched crystals, perpendicularly intersecting columns, assemblages of plates and/or side planes ------ with some cloud droplets attached"; at 1930 EST, "crystal types similar to 1910 EST but with heavy cloud droplet accumulations"; at 2045 EST, "crystal type(s) similar to 1930 EST but broken into finer particles by the wind". These observations indicate that a change in the characteristics of the snowfall did occur at ~ 1930 - 2030 EST with smaller sized particles of higher density (because of cloud droplet accumulations) being more prevalent after ~ 2000 EST.

Additional evidence of a change in snowfall characteristics can be obtained by analyzing the SRM and the ASCME data in a different manner. The natural dimensional units of snow rate are M/L^2T or grams (g) per length squared (L^2) per unit time (T). The units of LWC are g/L^3. Thus, if snow rate is divided by LWC, the resulting parameter has units of L/T and it is a measure of the average or integrated-fall velocity of the snowflakes (plus or minus the updraft-downdraft motion of the environmental air in the immediate vicinity of our sampling instrument, which we have presumed to be zero). The resultant fall-velocity values determined from the SRM data and ASCME No. 2 are shown plotted versus time in Fig. 7 (these are representative of the other two instruments). The plot shows that the integrated-snowfall velocities were smallest during the latter portion of the snowfall period when the LWC and snow-rate values were also smallest.

Also shown in the figure are the ranges of the fall-velocity values for individual snowflakes as determined from the FVI. Although range values are shown at ~ 2100 EST, an increase in wind velocity seriously impeded instrument operation after the 2000 EST IMP and we only managed to make a few (16) measurements from 2100-2115 EST. It is seen that the integrated or P/M-velocity values generally conform to the upper half of the range of the FVI measurements through the 2000 EST IMP and the lower portion of the 2100 EST IMP.

These measurements from the 2100 EST IMP period are plotted in Fig. 8 along with the regression and standard deviation lines from the individual-particle, fall-velocity measurements (Fig. 1) acquired prior to ~ 2100 EST. The individual particles from the latter period are of predominantly smaller sizes with velocities that generally fall below the solid regression line and the majority of the points are less than the lower standard deviation limit. The mean value of these measurements however, are slightly larger than the P/M fall-velocity determinations from the SRM and ASCME during the same time period.

Data obtained after ~ 2000 EST presents some conflicting evidence. For instance, ASCME data show mass concentrations at 1900 EST that are approximately comparable to those at 2100 EST. The precipitation rate is considerably lower at 2100 EST than at 1900 EST. Attenuation data show an increase at 2100 EST as compared to the 1900 EST measurement.

In order to justify a smaller snow rate with an increase in attenuation at the same value of M, one can postulate an increased number of particles of smaller sizes. This could also account for the smaller fall velocities. The reduction in snowflake size is substantiated by the CRREL observations noted during this period and confirmed by the FVI measurements in Fig. 8. However, the CRREL

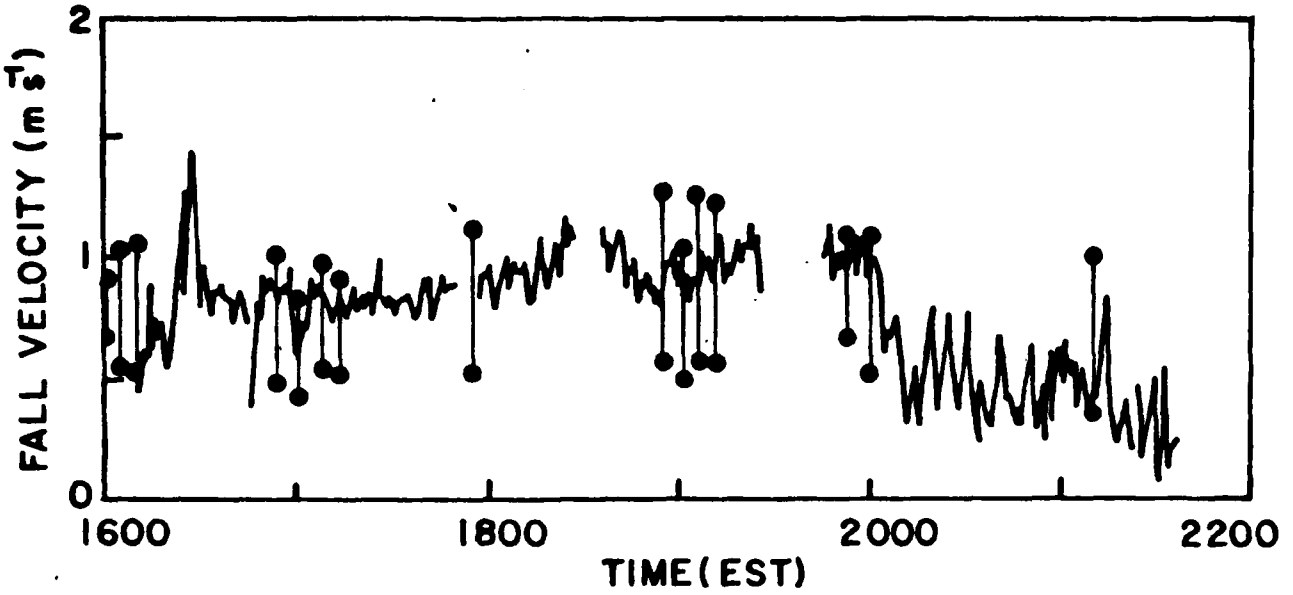

Fig. 7 Fall velocities derived from P and M for ASCME No. 2 on 31 Jan 82.

observations noted the accumulation of cloud droplets on these smaller, broken flakes. Since these minute water droplets would increase the particle density, one would expect an increase in fall velocity for given particle sizes which is contradictory to the data plotted in Fig. 8. One possible explanation is the increase in wind velocity at ~ 2000 EST may have produced updraft components of air motion over both the FVI and SRM instruments thus giving artificially-small, fall-velocity determinations.

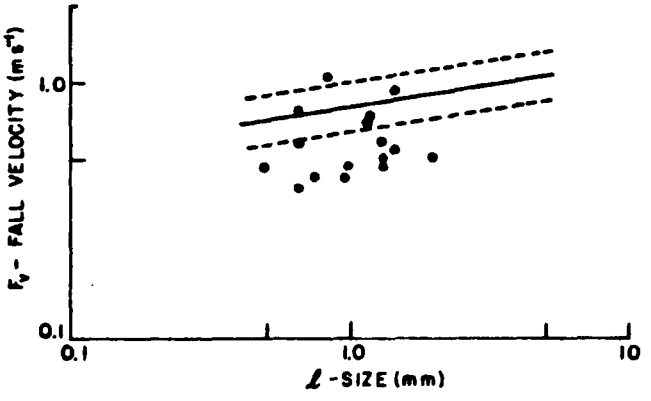

Fig. 8 Fall velocities of individual particles from 2100 to 2115 EST on 31 Jan 82.

3. SNOW-ONE-B FIELD EXPERIMENT

The SNOW-ONE-B fall velocity indicator was essentially the same instrument as used in SNOW-ONE-A. A minor modification was made in the electronics that controls the strobe lighting to insure the validity of the flash rates.

The snow-rate meter was modified during the summer months by reducing the distance (shaft length) between the collection bucket and the electronic balance remote sensing head. This alteration necessitated installation of a baffle between the bucket and heated chamber housing to insure against the possibility of escaping heat affecting the sample. The modification, although relatively minor, drastically changed the nature of the acquired data. The instrument configuration used in SNOW-ONE-A displayed wind effects that varied somewhat symmetrically about the weight measurements. The SNOW-ONE-B data displays a decidedly biased effect on the positive side of the weight measurements (downward force on the collection bucket) with little deflection on the negative side. This change required a totally new method of analysis that was described in the SNOW-ONE-B data report. This method of SRM analysis was used on the data of 31 Jan 82 for a comparison of the two methods. The first two hours of data are shown in Fig. 9 with the light line representing the parabolic-weighted averaging method used on the SNOW-ONE-A measurements and the heavy line showing the method used on the SNOW-ONE-B data. Very minor deviations are evident but they are so slight that the methods can be considered comparable.

The snow-structure recorder was extensively modified during the summer months. As mentioned previously, the device used during SNOW-ONE-A employed a continuously moving belt utilizing strobe lighting to provide "stop action". The SNOW-ONE-B instrument incorporates low-intensity, incandescent lighting with

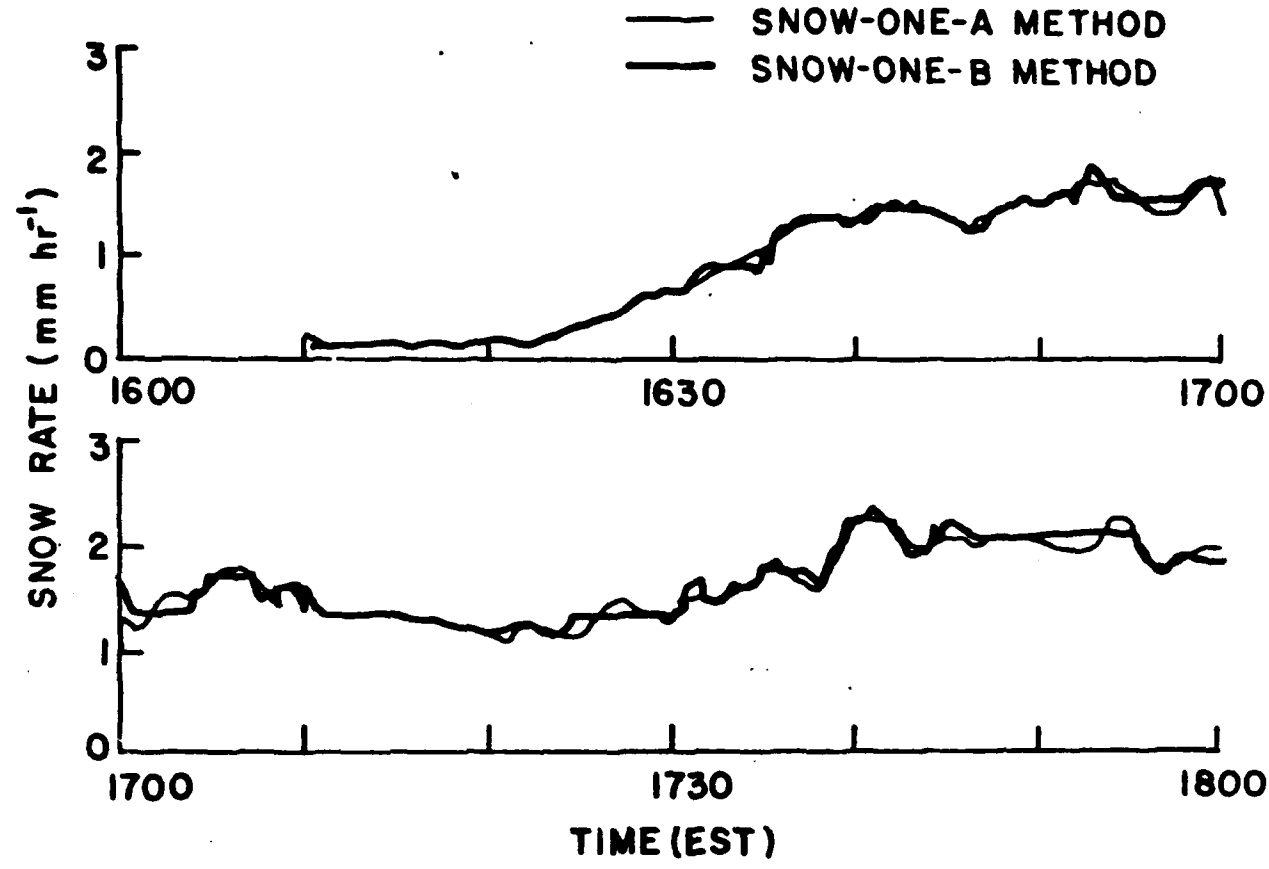

Fig. 9 Comparison of two analytical methods using data from 31 Jan 82.

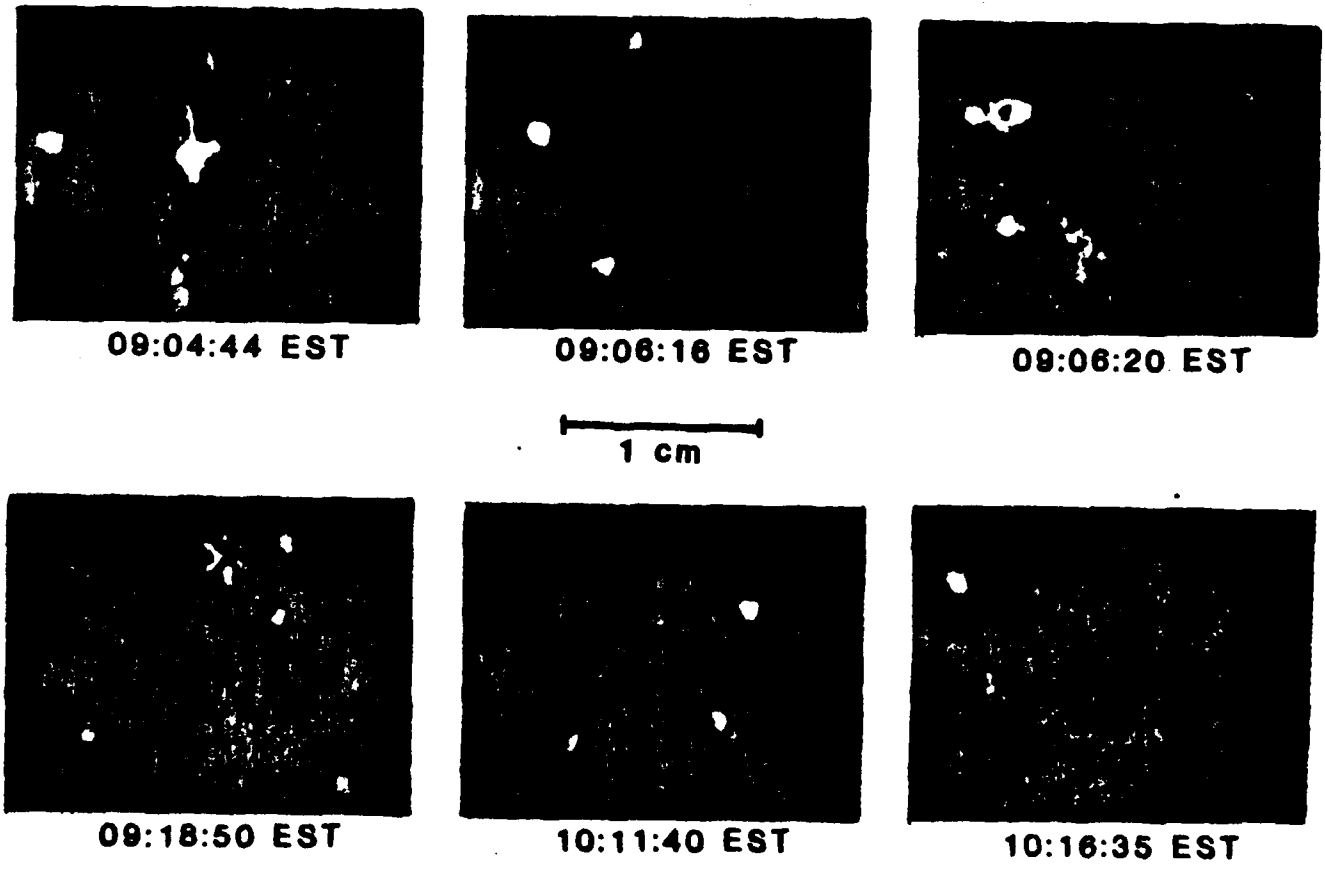

Fig. 10 Typical data obtained with the SSR on 12 Dec 82.

belt action in a "move and stop" sequence controlled by a geneva drive mechanism. Thus, recordings during this experiment were made under reduced lighting when the belt was stationary. The data results were much improved.

3.1 DATA OF DECEMBER 12, 1982

Of the six days of recorded snow-rate data during SNOW-ONE-B, 12 Dec 82 provided the most extensive period of snowfall during daylight hours. All instruments were turned on at 0855 EST and the SRM was left running until the end of the recording tape at 0230 EST on the 13th. The SSR and FVI were terminated at 1350 EST.

Analysis of the video recordings from the SSR revealed graupel-type particles mixed with larger stellars and dendrites. The constituents of the mix remained fairly consistant throughout the storm although the percentages of the particular types varied continuously. It is estimated that stellars and dendrites composed less than 10% of the particles that were sampled. Some examples of the particles captured by the SSR on this day are shown in Figure 10.

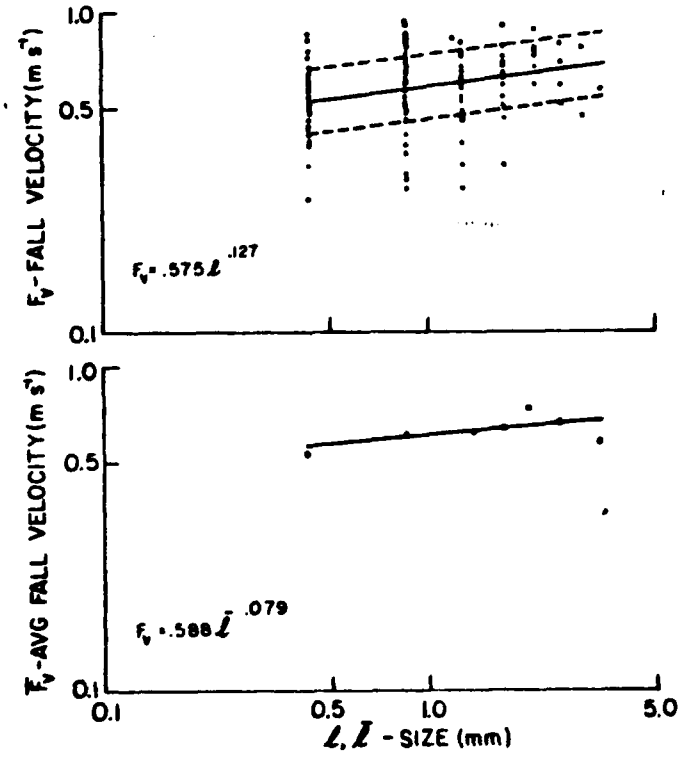

Fig. 11 Fall velocities of individual particles and class averaged on 12 Dec 82.

Because of the time-consuming labor necessary for the reduction of the FVI data, the initial analysis consisted only of representative recordings (50 measurements) taken within the times conforming to each intensive measurement period. Figure 11 (upper diagram) is a plot of fall velocity vs size for the individual particles over those time periods. The lower diagram shows the class-averaged-fall velocities plotted versus size in the same manner as described in Section 1.

The ASL/LOVIR (Ben-Shalom, A., et. al., 1983) transmittance measurements from 1000 to 1300 EST on 12 Dec 82 are shown in Fig. 12 along with our inversed snow-rate data. The casual time correlation is obvious. One ASCME instrument operated during this storm and we obtained the data through the courtesy of J. Lacombe (CRREL) for correlation with our SRM measurements. Figure 13 shows these two data sets with the light line representing the SRM and the heavy line, the ASCME. The snow-rate data has been averaged over 1 minute intervals to conform to the ASCME measurements. The general correlation is obvious although many inconsistancies are apparent, particularly at the very small concentrations and rates.

These inconsistencies are also evident in the considerable scatter shown in the 1 minute data plot of M vs P in the top diagram of Fig. 14. However, this scatter is quickly reduced when the data is subjected to a running-mean averaging as in the lower plots.

The scatter is more striking in the calculated P/M fall-velocity values of Fig. 15 but, as in the M - P plots, it is reduced by averaging. The most stable period is between 1025 and 1055 EST which are the time limits corresponding to the largest snowfall intensity (P = > .13, M = > .06). The second most stable region falls between 1005 and 1025 EST when P was ~ .1 and M ~ .02. All other times experienced less snowfall.

It is unclear, at this time, if the calculated P/M fall velocites between 1005 and 1025 EST (~ 1.2 m s^{-1}) are, in fact, real. The indications are that they may not be since no velocity above 1 m s^{-1} was observed in the measurements of the individual flakes (Fig. 11).

The 1000 EST IMP of 12 Dec 82 was divided in the same manner as the 1900 EST IMP of 31 Jan 82 to check both the fall velocities of the individual flakes and the consistancies of the $F_v - \ell$ relationships throughout the period. Because of the lesser amount of snow falling on this day, 50 particles were counted starting at 1000, 1005, 1010 and 1015 EST. The times over which these 50 measurements

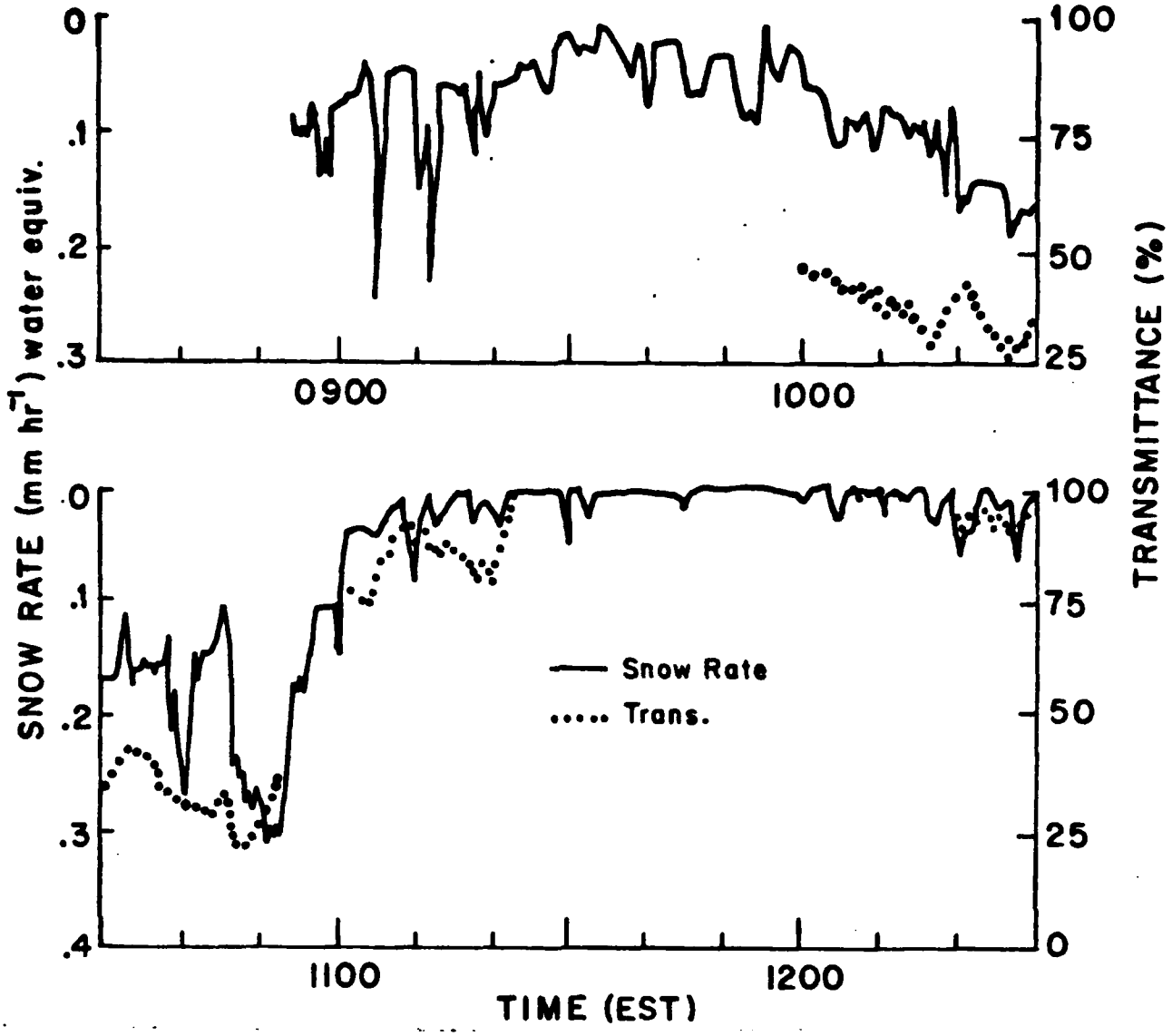

Fig. 12 Time comparison of ASL/LOVIR and snow rate data on 12 Dec 82.

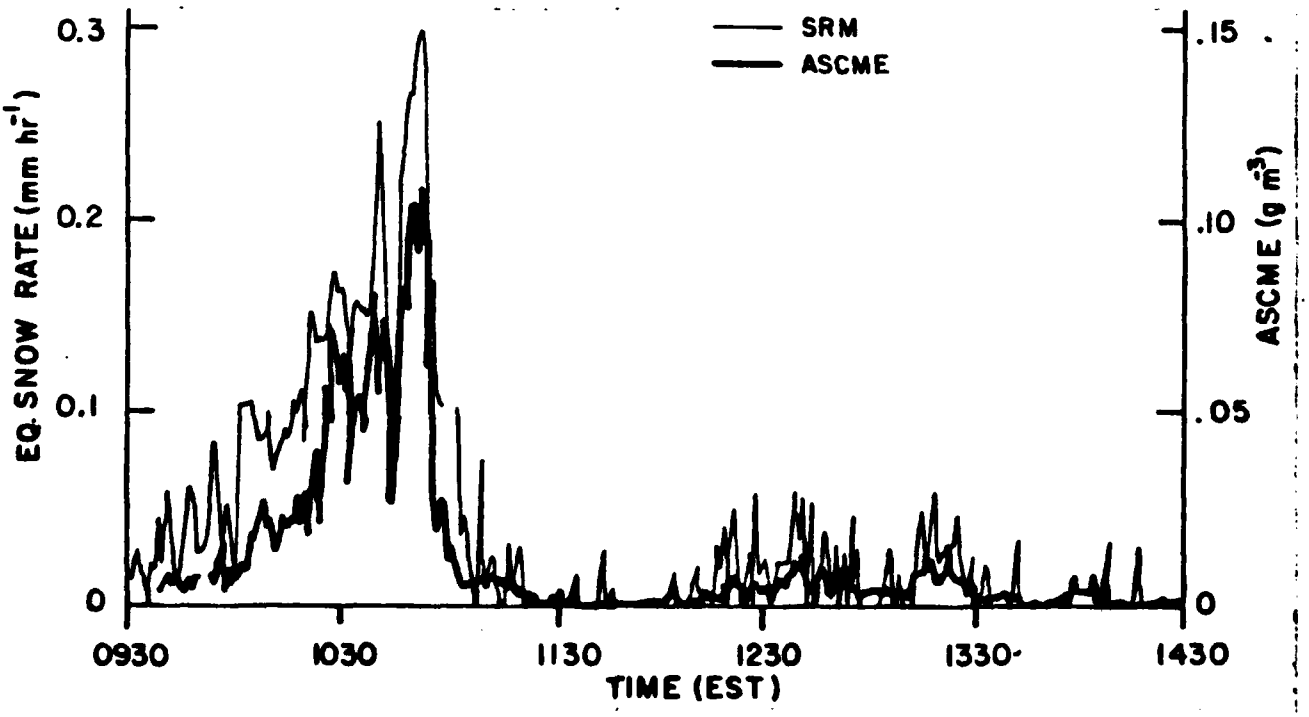

Fig. 13 Time comparison of ASCME and snow rate data on 12 Dec 82.

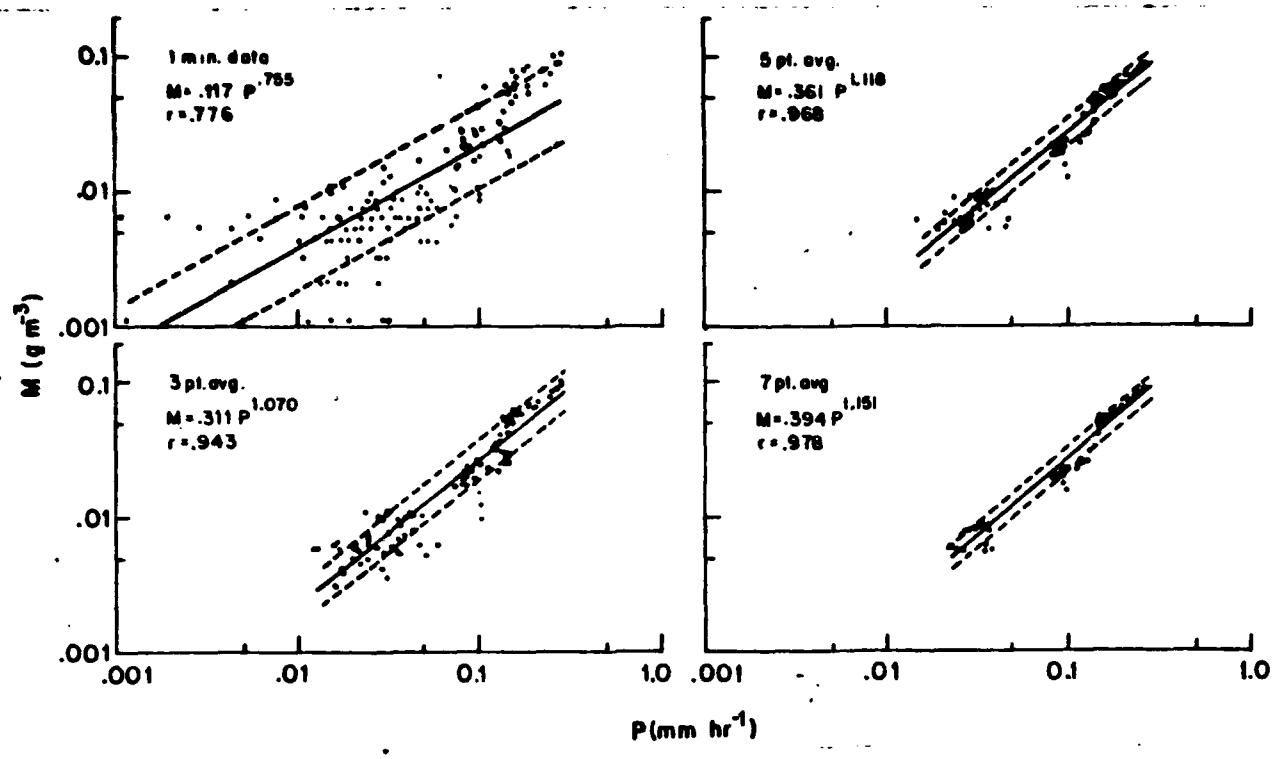

Fig. 14 Correlation of mass concentration and snow rate on 12 Dec 82.

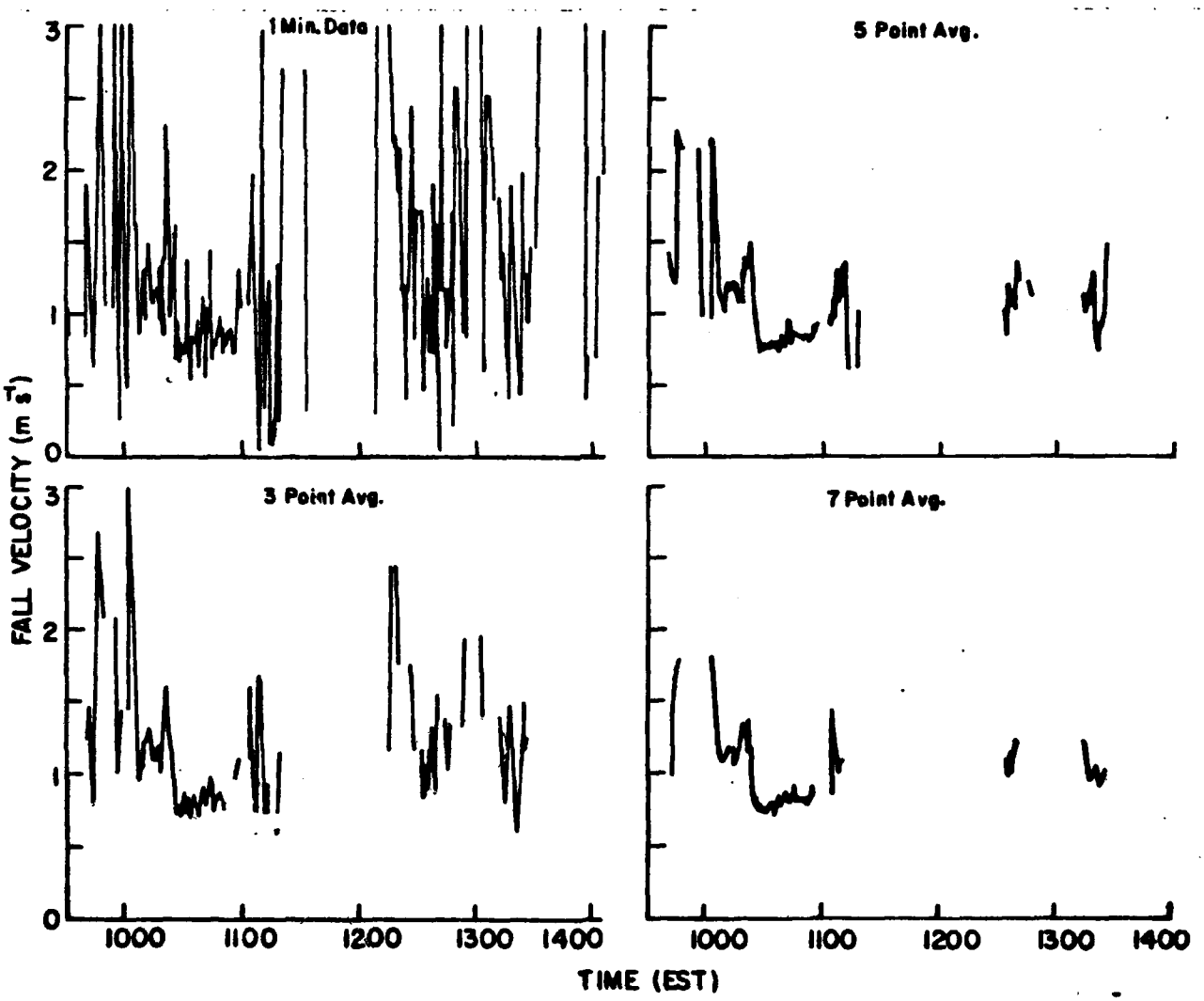

Fig. 15 Fall velocity derived from P and M on 12 Dec 82.

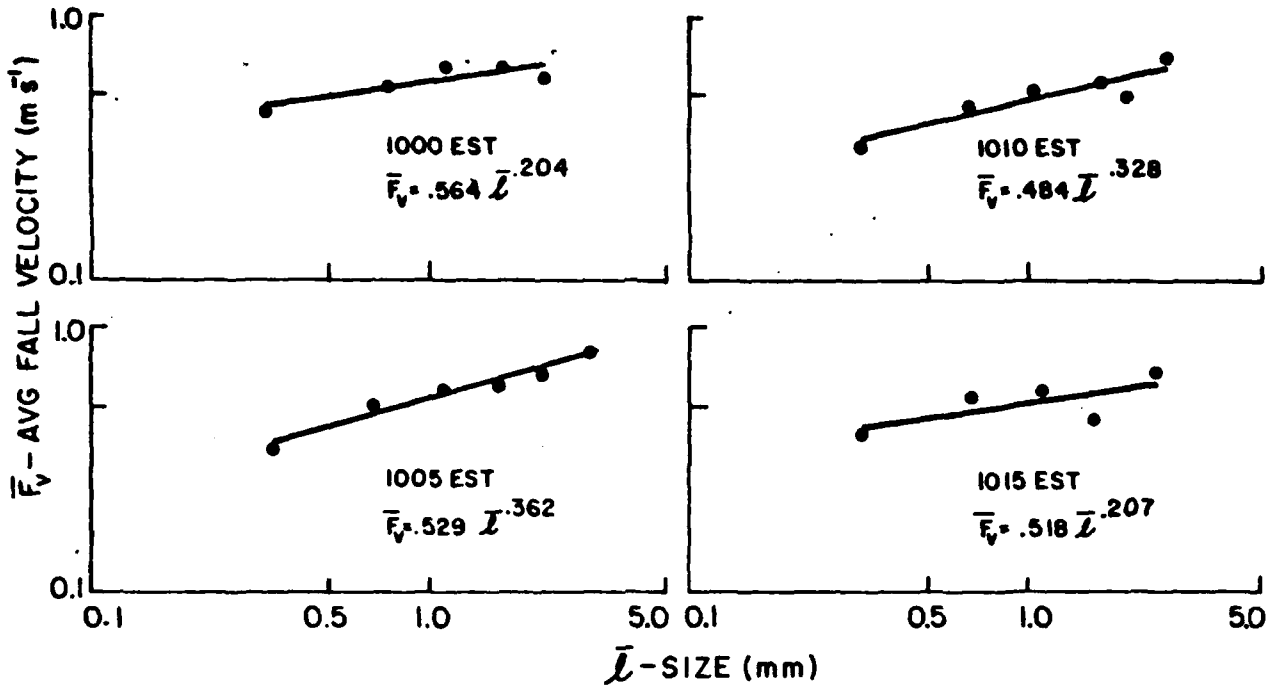

Fig. 16 Class-averaged-fall velocities from the 1000 EST IMP on 12 Dec 82.

were made ranged from ~ 4 to 5 minutes. Again, no reading > 1 m s^{-1} was recorded which adds evidence questioning the validity of the P/M fall velocities of Fig. 15 during the 1000 EST IMP.

The resulting regression equations presented in Fig. 16 are inconsistant indicating the changing nature of the snowfall during this period. All have steeper slopes than the equations derived from the composite IMP data set. This leads one to suspect that the data from at least one other IMP (or possibly more) produced a slope more shallow than that of the composite. This, in turn, suggests a variability in snow characteristics during the course of the storm and confirms the findings from the SSR.

As a check on the integrated velocities obtained from 1025 - 1055 EST we measured 50 individual flakes starting at 1030 EST. These measurements are plotted in Fig. 17 and the results of the analysis gives an equation compatible with the 1005 - 1010 EST period of Fig. 15. The mean value of .5 m s^{-1} from these individual velocities does not agree with the P/M values (~ .8 m s^{-1}).

The non-compatibilities mentioned above point to possible errors in the data supplied by 1, 2 or all 3 of the instruments (FVI, SRM or ASCME) involved in these analyses. Several scenarios are possible such as:

(a) a wind effect (updraft) on the FVI could result in low fall velocities;
(b) the same wind effect on the SRM could cause low rate values and, since the integrated-fall velocities are determined by P/M, the resultant velocities would be high;
(c) lower than actual values from the ASCME could cause higher integrated-fall velocities.

It must be emphasized that we have not defined a source of error. At this time, we can only bring attention to the inconsistancies which seem to indicate measurement error.

4. CONCLUSION

Modifications made to our instruments during the summer months following SNOW-ONE-A have greatly contributed to an improved performance as demonstrated in SNOW-ONE-B. We are conducting further modifications that we hope will still better our measurements. A new concept of back lighting on the FVI, that gives shadow recordings of the falling snowflakes, is currently undergoing laboratory testing and promises sharper video images, thus more accurate measurements. The SSR is also being reconfigured to improve collection efficiency. A snow volume recorder and a total number instrument are also being considered.

The data acquired during SNOW-ONE-A & B raised questions regarding wind effects and the accuracy of light precipitation determinations. We are planning to conduct some airflow studies under varying wind conditions on both the FVI and SRM that may provide some useful informa-

tion. However, until we can define a fault in the SRM operation in light snow conditions, we can only tentatively presume the readings to be correct.

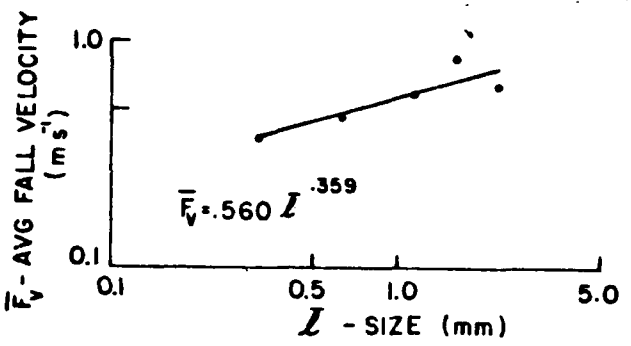

Fig. 17 Class-averaged-fall velocities from 1030 to 1035 EST on 12 Dec 82.

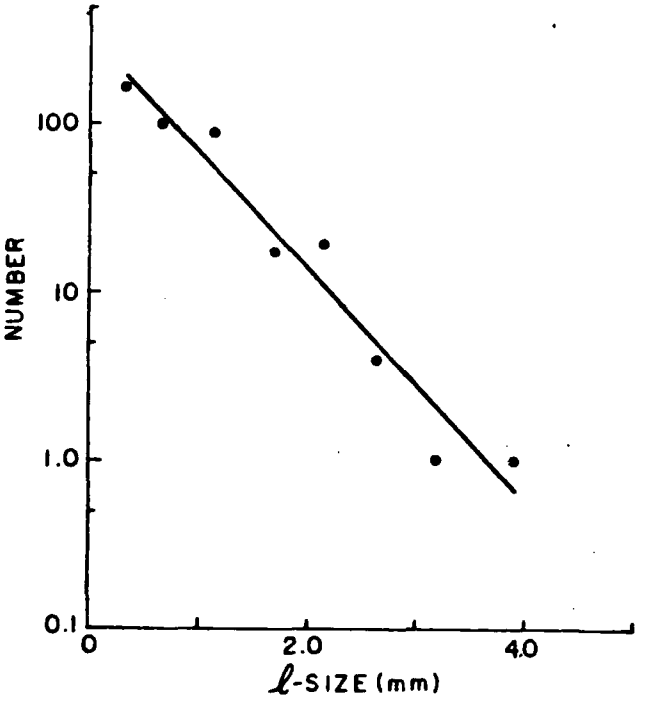

Fig. 18 Number density distribution from the FVI data of the 1900 EST IMP on 31 Jan 82.

In the process of developing class-averaged-fall velocities using the 400 individual snowflake measurements from the 1900 EST IMP on 31 Jan 82 and the 200 from the 1000 EST IMP on 12 Dec 82, we also produced the number of particles contained within each size class. When these number densities are plotted versus the mid-class values of the particle's longest dimension in a semi-logarithmic format (Figs. 18 and 19), they show a general conformity to an exponential shape. This agrees with our past findings using aircraft acquired data and raises the possibility of estimating realistic number-density distributions using the exponential assumption in combination with data supplied by the available ground-based measurements. Theoretical work along these lines is currently in progress.

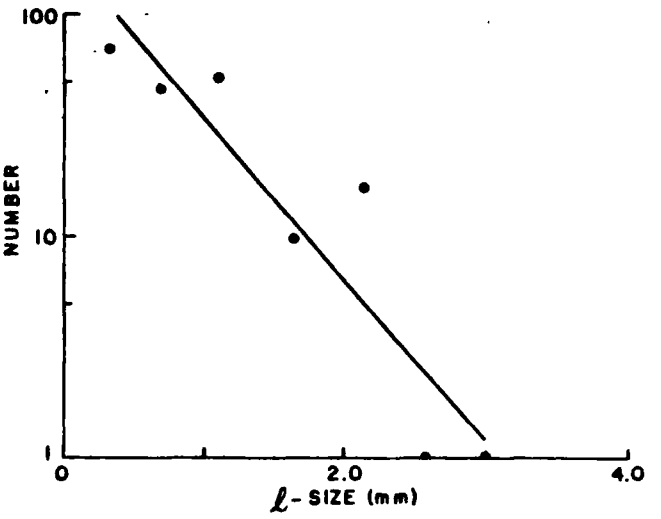

Fig. 19 Number density distribution from the FVI data of the 1000 EST IMP on 12 Dec 82.

ACKNOWLEDGEMENTS

The authors wish to thank Susan Sadofsky for her work in reducing the FVI data and to Don McLeod for the SSR data. A special thanks to Anthony Matthews, SMSgt. Stephen Crist and SSgt. Dennis LaGross for their operation of the equipment.

REFERENCES

Berthel, R.O. (1982), Snow characterization measurements at SNOW-ONE-A, SNOW-ONE-A DATA REPORT, U.S. Army Corps of Engineers, CRREL Special Report 82-2, 421-437, AFGL-TR-82-0003, ADA 118140.

Berthel, R.O., Plank, V.G. and Main, B.A. (1983), AFGL snow characterization measurements at SNOW-ONE-B: preliminary report, SNOW-ONE-B DATA REPORT, U.S. Army Corps of Engineers, CRREL Special report 83-16, 197-208, AFGL-TR-83-0174.

Berthel, R.O., Plank, V.G. and Matthews, A.J. (1982), AFGL snow characterization measurements at SNOW-ONE-A, Reprints of Snow Symposium II, CRREL, Hanover, NH, Aug 10-12, 35-48, AFGL-TR-83-0121.

Plank, V.G., Berthel, R.O. and Main, B.A., (1983): Snow characterization measurements and E/O correlations obtained during SNOW-ONE-A and SNOW-ONE-B, SPIE Technical Symposium East 83, Session "Optical Engineering for Cold Environments", Sub-session "Electro-Optical/Infrared Systems and Effects".

Plank, V.G., Matthews, A.J. and Berthel, R.O., (1983): Instruments used for snow characterization in support of SNOW-ONE-A and SNOW-ONE-B, SPIE Technical Symposium East 83 Proceedings, Session "Optical Engineering for Cold Environments", Sub-session "Optical Hardware in the Cold."

Gibbons, L.C., Matthews, A.J., Berthel, R.O. and Plank, V.G. (1983), Snow characterization instruments, Instrument Papers No. 316, AFGL-TR-83-0063.

Bates, R. (1982), Meteorology, SNOW-ONE-A DATA REPORT, U.S. Army Corps of Engineers, CRREL Special Report 82-8, 43-180.

Olsen, R., Okrasinski, R. and Brown, D. (1982), TACS data report for SNOWONE-A, SNOW-ONE-A DATA REPORT, U.S. Army Corps of Engineers, CRREL Special Report 82-8, 181-216.

Lacombe, J. (1982), Measurements of air borne-snow concentration, SNOW-ONE-A DATA REPORT, U.S. Army Corps of Engineers, CRREL Special Report 82-8, 225-282.

Koh, G. and O'Brien, H. (1982), Snow crystal habit, SNOW-ONE-A DATA REPORT, U.S. Army Corps of Engineers, CRREL Special Report 82-8, 181-216.

Ben-Shalom, A., Okrasinski, R., Olsen, R. and Butterfield, J.G. (1983), Visible/IR transmission and meteorology data, SNOW-ONE-B DATA REPORT, U.S. Army Corps of Engineers, CRREL Special Report 83-16, 89-154.

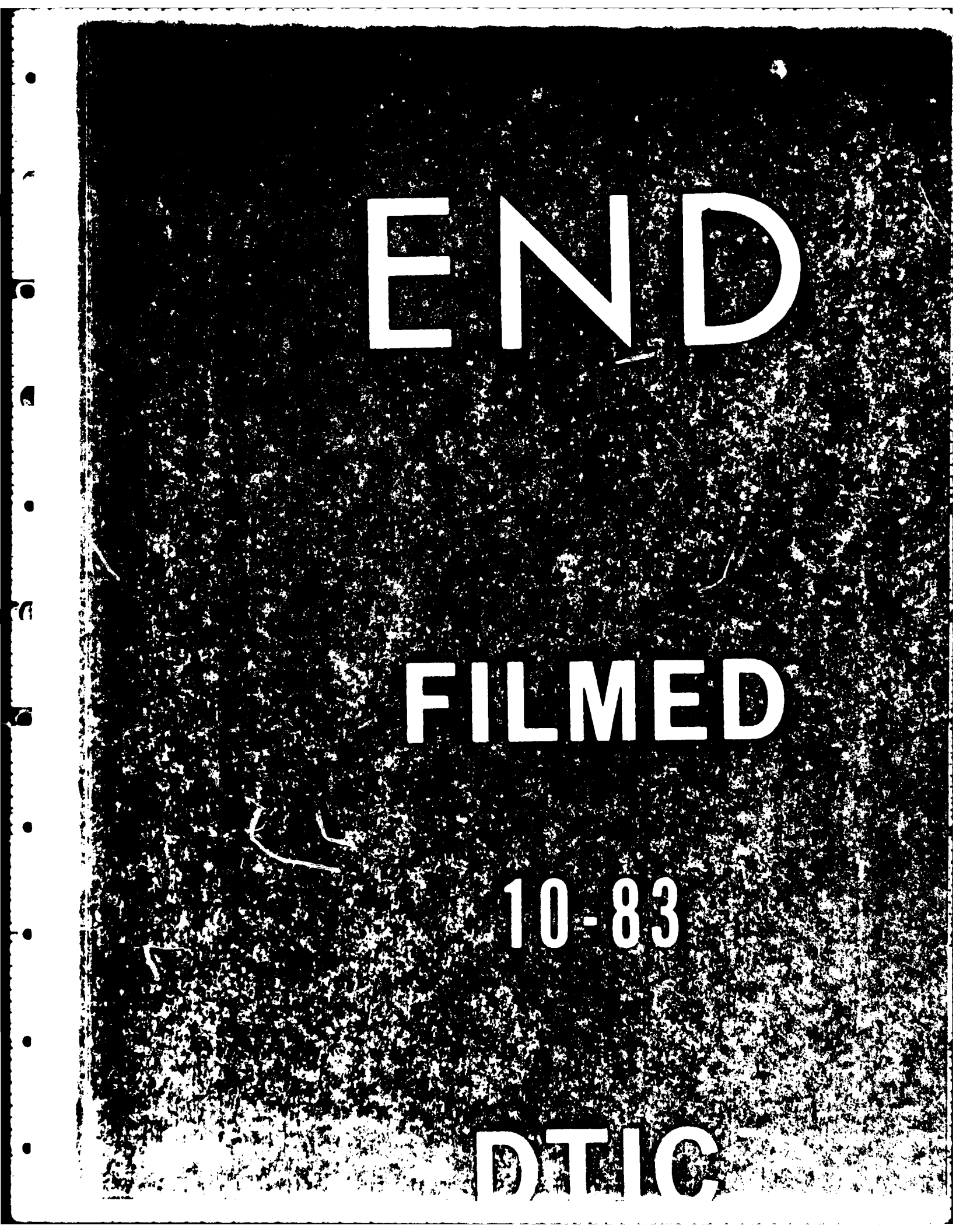
END
FILMED
10-83
DTIC